

## Vortex properties of $\text{YBa}_2\text{Cu}_3\text{O}_7$ superconducting thin films: Irreversible magnetization and the effect of thickness

Chang Jun Liu and Claire Schlenker

*Laboratoire d'Etudes des Propriétés Electroniques des Solides, associated with Université Joseph Fourier,  
Centre National de la Recherche Scientifique, Boîte Postale 166, 38042 Grenoble Cedex 9, France*

Jürgen Schubert and Bernd Stritzker\*

*Institut für Schicht und Ionentechnik, Forschungszentrum Jülich GmbH, Postfach 1913, D-W52425, Jülich, Germany*

(Received 21 September 1992; revised manuscript received 24 May 1993)

Magnetic properties of epitaxial thin films of  $\text{YBa}_2\text{Cu}_3\text{O}_7$  have been studied in the superconducting state in fields perpendicular to the sample, along the  $c$  crystallographic axis. In the low-temperature state, susceptibility, hysteresis loop, and remanent magnetization (trapped flux) studies show that a critical state is established in very low applied fields. The flux penetration process and the related thickness properties are well accounted for by simple electromagnetic models for the critical current. It is shown that the evaluation of the critical current  $J_c$  by the classical Bean formula is roughly valid, in spite of the curvature of the vortices. A decrease in the low-temperature value of  $J_c$  with increasing thickness is found above 100 nm. In the temperature range close to  $T_c$ , the irreversibility line moves towards higher field with increasing thickness according to a  $d^{1/2}$  law. This is discussed in relation with the theories of vortex-lattice and vortex-glass melting.

### I. INTRODUCTION

Since the discovery of the high- $T_c$  superconductors,<sup>1</sup> thin films of these materials have been extensively studied. Various techniques have been developed, especially to elaborate  $\text{YBa}_2\text{Cu}_3\text{O}_7$  thin films. Very soon, high-quality epitaxial films could be obtained.<sup>2,3</sup> The interest in thin films was stimulated by possible applications using transport or microwave properties. However, the geometry of thin films, with a thickness often comparable to the London penetration depth, provides means of studying special physical properties. For example, the role of surfaces or defects created by irradiation can be more easily studied on thin films.

Most of the studies performed on high- $T_c$  thin films are related to the elaboration techniques, the characterization of the samples, and the transport properties in the superconducting state, without or with an applied magnetic field. However, comparatively few detailed studies concern their magnetic properties, although these properties have been extensively studied on bulk materials, ceramic, or single crystals.<sup>4</sup>

One of the major problems of type-II superconductors concerns the mechanisms of flux penetration and flux pinning in the mixed state.<sup>5</sup> The value of the critical current, an important parameter for applications, is directly related to the flux-pinning properties.<sup>6</sup> Transport measurements alone cannot clarify this point. It is also necessary to collect magnetic data that are more directly related to the flux properties.

The relation between critical current  $J_c$  and magnetization has been established by Bean, on the basis of the notion of what is now called the critical state.<sup>7</sup> The Bean formulas, which simply connect the remanent magnetiza-

tion to  $J_c$ , are commonly used since they provide an easy method to evaluate  $J_c$  through magnetic measurements without contacts. However, the Bean formulas are strictly valid for "infinite" samples with the magnetic field applied along a long dimension. This is not the case of a thin film with field applied perpendicular to its plane, where the demagnetizing field effects are dominant. Detailed magnetic studies combined with electromagnetic calculations can clarify this point and especially estimate the importance of the curvature of vortices in this configuration.

$\text{YBa}_2\text{Cu}_3\text{O}_7$  thin films show comparatively high critical currents, in the range of  $10^{11}$  A m<sup>-2</sup> at low temperature.<sup>2,3</sup> The origin of the strong pinning of vortices responsible for such high  $J_c$  is not clear at the moment. The nature of defects, the role of surface pinning, and more generally, of intrinsic pinning due to the quasi-two-dimensional properties of these materials, are not established now. In the case of these films, one can vary one parameter, the film thickness. Studies of the pinning properties on epitaxial thin films with different thicknesses could bring new information that could contribute to the understanding of the mechanism of pinning.

High- $T_c$  superconductors are characterized by the so-called irreversibility line, which corresponds to the presence of a reversible regime and therefore, to the vanishing of critical current below  $T_c$  in field  $H_{irr}$ , much smaller than the higher critical field  $H_{c2}$ .<sup>8</sup> This was established in the pioneering work of Müller, Takashige, and Bednorz, through measurements of the so-called zero-field-cooled and field-cooled magnetization on a  $(\text{LaBa})\text{CuO}_{4-y}$  ceramic.<sup>8</sup> The observed metastable properties were then attributed to the existence of a superconducting glass state, possibly associated with granular

properties of the materials. Soon after, similar results were obtained on  $\text{YBa}_2\text{Cu}_3\text{O}_7$  single crystals by Yeshurun and Malozemoff.<sup>9</sup> The existence of the vanishing of the flux pinning, and therefore, of the irreversible properties on the irreversibility line was accounted for by giant flux-creep phenomena, due to comparatively small pinning and large thermal energies, in the special case of high- $T_c$  superconductors. The possibility of a superconducting glass state, due to the existence of disordered pinning centers destroying the long-range order of the Abrikosov vortex lattice, was proposed later by Fisher.<sup>10</sup> In this context, the irreversibility line could be attributed to a transition from a vortex-glass state to a vortex-liquid state. Simultaneously, models involving the melting of the vortex lattice were proposed by Nelson and Seung<sup>11</sup> and by Brandt.<sup>12</sup> Such melting has been previously analyzed for thin films of conventional type-II superconductors, with a thickness smaller than the London penetration depth.<sup>13</sup> It has been argued that the effect of thermal fluctuations could lead to a melting transition similar to the Kosterlitz-Thouless transition predicted for two-dimensional systems.<sup>14</sup> In the case of the high- $T_c$  superconductors, it is believed that vortex-lattice melting could occur due to high accessible temperatures and therefore, to large thermal fluctuations. This may be described on the basis of the elastic properties of the vortex lattice, applying the Lindemann criterion for melting to the mean-square value of the vortex-lattice displacements (for review see Refs. 15 and 16). Whether the related irreversibility line corresponds to a vortex-glass or a vortex-lattice transition is still an open question.

From an experimental point of view, the irreversibility line can be obtained by transport, by magnetization, or by mechanical measurements. In the case of thin films, previous results had been obtained by the studies of current-voltage characteristics and supported the model of the vortex-glass state.<sup>17</sup> The energy dissipation due to flux-line motion has also been studied by means of a mechanical oscillator, leading to results consistent with a vortex-glass state.<sup>18</sup> While many results have been obtained by magnetic measurements on single crystals, we are not aware of such data on thin films.

Magnetization studies can provide the irreversibility line either by comparison of the thermal dependence of field-cooled and zero-field-cooled magnetizations, as was done in Ref. 8, or by the direct measurement of the irreversible magnetization on the hysteresis loops recorded at different temperatures. We have used this second method to study the irreversibility line of films of different thicknesses. Such studies are of special interest, since the film thickness is comparable to the London penetration depth ( $\lambda_L = 140$  nm for fields parallel to the  $ab$  plane) and may also be comparable to some correlation length along the flux lines.

One should note that detailed studies of the hysteresis loops at different temperatures also give information on the field and temperature dependence of the critical current. These properties are directly related to the flux-pinning mechanisms and to flux-creep phenomena, which are known to be especially important in high- $T_c$  superconductors. The problems related to flux pinning and

flux creep have also stimulated considerable amounts of work. The classical model for flux creep, due to Anderson and Kim,<sup>19</sup> is based on the thermal motion of uncorrelated vortices of vortex bundles over a potential barrier of height  $U_j$ , which depends linearly on the applied current  $J$ . Other models involve a collective vortex pinning mechanism, first proposed by Larkin and Ovchinnikov.<sup>20</sup> This assumes a strong deformation of the vortex lattice due to the presence of a large concentration of randomly arranged pinning centers. This model leads to the concept of a correlation volume  $V_c$ , in which the vortex lattice is nearly perfect. Outside this volume, there is no long-range order due to the presence of pinning centers. This mechanism of pinning is clearly closely related to the concept of the vortex-glass state.<sup>10,16</sup> The theories for flux creep based on the collective flux-pinning mechanism<sup>21</sup> lead to an inverse power law for the current dependence of the barrier energy, typically  $U_j \sim J^{-\alpha}$ , where  $\alpha$  is an exponent of the order of unity depending mainly on the size of the vortex bundle involved in the creep phenomenon.

One should note that in these models, the basic concept of the correlation volume involves two characteristic lengths, the transverse one  $R_c$  and the longitudinal one  $L_c$ , perpendicular and parallel, respectively, to the magnetic field. It is clear that in the case of thin films in perpendicular applied fields, the order of magnitude of the longitudinal correlation length  $L_c$ , as compared to the film thickness, will be of special importance.

In this context, we have performed detailed studies of the magnetic properties in the superconducting state of  $\text{YBa}_2\text{Cu}_3\text{O}_7$  epitaxial films grown by laser ablation on  $\text{SrTiO}_3$  substrates. Films with thickness in the range 50–400 nm have been measured. We have focused our work on the properties of the initial (virgin) magnetization curve, the hysteresis loops, and remanent magnetization for different values of the maximum applied field,<sup>22–24</sup> as well as on the irreversibility line.<sup>24</sup>

This paper is organized as follows. In Sec. II we describe the experimental techniques. In Sec. III we report results on the initial magnetization, low-field initial susceptibility, and differential reverse susceptibility. Section IV is devoted to the hysteresis-loop and remanent-magnetization (trapped-flux) studies. In Sec. V, we give the results obtained for the irreversibility line. Finally, in Sec. VI, we extract some conclusions from this work.

## II. EXPERIMENTAL TECHNIQUES

$\text{YBa}_2\text{Cu}_3\text{O}_7$  thin films have been prepared by laser ablation, using a pulsed excimer laser and a cylindrical rotating target without post annealing, as described in Refs. 25 and 26. The technique assures homogeneous ablation on large substrates. The films were deposited on (100)-oriented single crystal  $\text{SrTiO}_3$  substrates, maintained at a temperature between 600° and 780°C. The target was a stoichiometric sintered  $\text{YBa}_2\text{Cu}_3\text{O}_7$  sample. The critical temperature  $T_c$  was found above 88 K for all films of thicknesses larger than 10 nm. All samples showed a metallic resistivity above 90 K of the order of 0.3 mΩ cm at 300 K. The thickness of the film was measured by the

Rutherford backscattering (RBS) technique with an absolute accuracy of 5%. The room-temperature resistivity was found to be independent of the thickness within this accuracy between 50 and 200 nm. Critical currents were found to be in the range of  $10^{10}$  A/m<sup>2</sup> at 77 K for film thicknesses above 50 nm.

The structural properties were characterized mainly by He ion channeling. The content of Ba, Cu, and Y, obtained from RBS, was the same as in the stoichiometric target. The minimum backscattering yield  $\chi_{\min}$  for a 2 MeV He beam perpendicular to the film was found to be smaller than 10% and independent of thickness. X-ray studies established that the *c* axis was perpendicular to the film. These results, together with  $\chi_{\min}$  values for different orientations of the He beam, established that the films are epitaxial, with excellent *c*-axis orientation perpendicular to the films and a good crystalline alignment in the plane of growth. This does not exclude twinning in the *ab* plane.

Scanning electron microscopy studies showed that the samples were smooth, except for some small particles of 0.2  $\mu\text{m}$  diameter, with a chemical composition between  $\text{YBa}_2\text{Cu}_3\text{O}_7$  and CuO. These particles do not seem to influence the electrical properties. Table I gives the thickness and onset critical temperature  $T_c$  of the studied samples.

The magnetic measurements were performed with a vibrating-sample magnetometer built in the Laboratory. A magnetic field, up to 6 T, is provided by a superconducting magnet. The amplitude of the vibration was 1 mm for all measurements and its frequency was 67 Hz. The high sensitivity of the apparatus (magnetic moment of  $10^{-9}$  A/m<sup>2</sup> or  $10^{-6}$  emu) is obtained with pickup coils immersed in liquid helium and located close to the samples. For low-field measurements (0.1 mT), zero-field calibration was obtained by using a lead reference sample in its superconducting state.

The results reported here have been obtained with the magnetic field perpendicular to the sample. The samples were cut in the shape of squares or rectangles close to the size  $4 \times 4$  mm<sup>2</sup>. For hysteresis-loop and remanent-magnetization measurements, the sample was warmed up to 100 K between successive measurements and cooled

TABLE I. Characteristics of some of the investigated samples. Only samples 15, 16, 17, and 18 have been deposited from the same target in the same set of experiments. Other samples correspond to different experiments. Most of the reported results have been obtained on samples 15–18.

Sample	Thickness (nm)	$T_c$ (K) (determined on the zero-field-cooled magnetization curves)
1	400	89.0
7	100	88.0
9	200	89.0
11	400	89.3
15	200	91.8
16	150	91.5
17	100	91.1
18	50	88.8

again in zero field in order to suppress previously trapped flux.<sup>27</sup>

### III. INITIAL MAGNETIZATION, INITIAL AND DIFFERENTIAL REVERSE SUSCEPTIBILITIES

#### A. Experimental results

Figure 1 shows typical results for the initial magnetization  $M$  as a function of the applied field  $H_0$ , obtained after zero-field cooling, for several films with different thicknesses. The applied field  $H_0$  was always perpendicular to the sample. One notes that the initial susceptibility  $\chi_i$ , obtained in low fields ( $H_0 < 5000$  A/m<sup>-1</sup> =  $1.25 \times 10^{-2}$  Oe), is in the range of  $10^4$  and is decreasing with increasing thickness  $d$ . The curves also show a maximum of  $M$  for a field  $H_B$  that increases with  $d$ .  $H_B$  is related to the full penetration field. Its increase with the thickness is consistent with results obtained in Sec. IV and will be discussed in this context.

Figure 2 shows the initial susceptibility as a function of the geometrical factor  $R/d$ .  $R$  is an equivalent radius calculated from the in-plane dimensions  $l_1$  and  $l_2$  of the film through the formula  $\pi R^2 = l_1 l_2$ . If one assumes a linear variation of  $\chi_i$  and  $R/d$ , one obtains  $\chi_i \sim 0.8R/d$ .

Figure 3 shows typical hysteresis loops obtained for increasing values of the maximum applied field  $B_0^m$  ( $B_0^m = \mu_0 H_0^m$ ), for comparatively small values of  $B_0^m$  ( $< 100$  mT). It is clear in this figure that the differential susceptibility on the reverse leg of the hysteresis loop at  $H_0^m$ ,  $\chi_d(H_0^m)$  is similar to the initial susceptibility  $\chi_i$ . This is a general result;  $\chi_d(H_0^m)$  is independent of  $H_0^m$  and equal to the initial susceptibility for all epitaxial films.

Figure 4 shows this differential reverse susceptibility as a function of  $B_0^m$  together with  $\chi_i$ ; there is clearly no variation of  $\chi_d(H_0^m)$  with increasing maximum applied field.

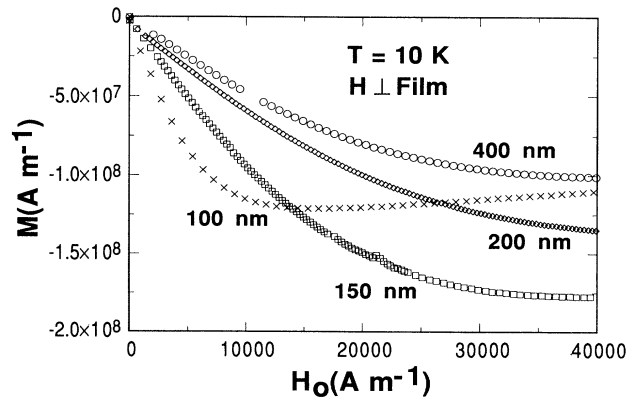


FIG. 1. Typical results for the initial magnetization vs magnetic field at 10 K for different film thicknesses. The in-plane sample dimensions were in the range  $4 \times 4$  mm<sup>2</sup>– $5 \times 5$  mm<sup>2</sup>. Applied field  $H_0$  perpendicular to the film plane.

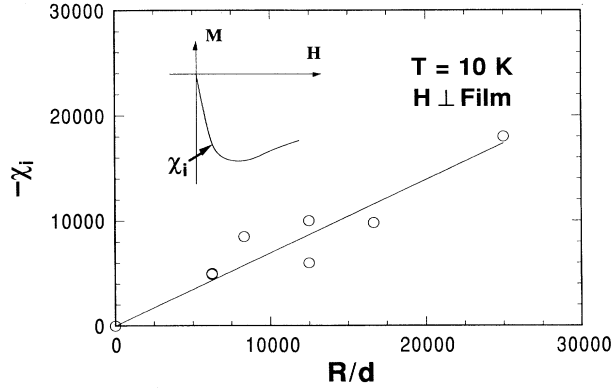


FIG. 2. Low-field initial susceptibility  $\chi_i$  as a function of the geometrical ratio  $R/d$ .  $R$  is the equivalent film radius and  $d$  the thickness.

### B. Discussion

Let us discuss the initial susceptibility  $\chi_i$ . We will first assume that the sample is in the Meissner state in low applied fields after zero-field cooling. If this would be the case, the initial susceptibility would be characteristic of the Meissner state. To evaluate the Meissner susceptibility of a thin film, one has to take into account demagnetizing field effects. For that, one can compare the sample to an oblate spheroid of semiaxis  $a = b = R, c = d/2$ . The demagnetizing field coefficient along  $c$  is found to be<sup>28</sup>

$$n_c = 1 - \epsilon, \quad \text{with } \epsilon \simeq \frac{\pi d}{4 R}.$$

Then, the internal field  $H$  would be such that

$$H = H_0 - nM = H_0 - n\chi H,$$

where  $H_0$  is the applied field and  $\chi$  the diamagnetic Meissner susceptibility expected to be equal to  $-1$ .

The apparent susceptibility would, therefore, be

$$\chi_a = \frac{M}{H_0} = \frac{M}{(1+n\chi)H} = \frac{-1}{(1+n\chi)} = -\frac{4}{\pi} \frac{R}{d}.$$

$\chi_a$  would be decreasing with increasing thickness as experimentally observed. However, if one evaluates the internal field  $H$ , one obtains

$$H \simeq \frac{H_0}{(1+n\chi)} \simeq \frac{H_0}{\epsilon}.$$

For a thin film 100 nm thick, the factor  $R/d$  is in the range of  $10^4$  and the internal field would be typically  $10^4$  times larger than the applied field. In most experimental cases,  $H$  would be larger than the lower critical field  $H_{c1}$  of  $\text{YBa}_2\text{Cu}_3\text{O}_7$  since  $\mu_0 H_{c1}$  is of the order 0.1 T along the  $c$  axis at low temperature.<sup>29</sup> This establishes that even in very low perpendicular applied fields, the film is not in the Meissner state. This is consistent with previous analyses for films of thicknesses comparable or larger than the London penetration depth.<sup>30</sup>

The experimental data which show that the initial susceptibility  $\chi_i$  is the same as the differential reverse susceptibility  $\chi(H_0^m)$  also support this result. Since for  $H = H_0^m$ , the film is clearly in the critical state, the experimental results indicate that the initial susceptibility  $\chi_i$  is also characteristic of a critical state. The experimental observations of flux penetration in a thin film by use of the Faraday effect are consistent with this analysis.<sup>31</sup> They show that in low applied field, flux enters first on the sides of the film in a narrow region which must be in the critical state.

The differential reverse susceptibility  $\chi_d(H_0^m)$  has been previously evaluated by Angadi *et al.*<sup>32</sup> in the case of a sample in the critical state. By imposing the conservation of the magnetic flux in the middle of the film, they obtained

$$\chi(H_0^m) \simeq -\frac{\pi R}{\theta d}, \quad \text{with } \theta = \ln \left[ 8 \frac{R}{d} \right] - \frac{1}{2}.$$

This assumes that the critical current circulates along the whole film. For a thin film, the parameter  $\theta$  is weakly dependent on the geometrical factor and  $\theta \simeq 11$ .

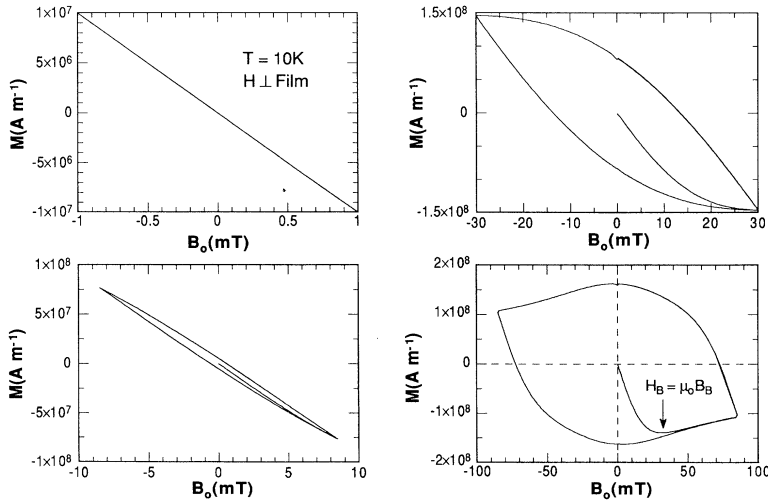


FIG. 3. Typical initial magnetization curves and low-field hysteresis loops for several values of the maximum applied field  $B_0^m$ .  $T = 10$  K,  $H \perp$  film,  $d = 200$  nm.

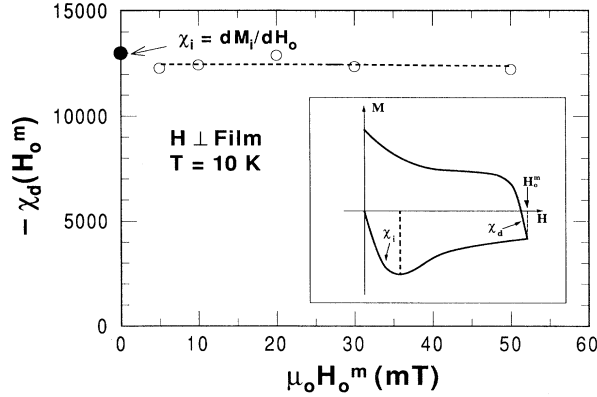


FIG. 4. Reverse differential susceptibility  $\chi_d H_0^m$  measured in decreasing fields from the maximum applied field  $H_0^m$ , as a function of  $\mu_0 H_0^m d = 200$  nm. (○) corresponds to the low-field initial susceptibility  $\chi_i$ .  $T = 10$  K,  $H \perp$  film.

Our experimental data correspond to

$$\chi_d(H_0^m) = -(0.8 \pm 0.4)R/d.$$

They are not too far from the predicted theoretical value.

One can extend the model of Angadi *et al.* to evaluate the initial susceptibility  $\chi_i$ , if one assumes the outer part of the film to be in the critical state in low applied fields. The predicted value of  $\chi_i$  is then the same as  $\chi(H_0^m)$ , if one performs the same type of calculation,

$$\chi_i = (\chi_0^m) = -\frac{\pi R}{\theta d}.$$

Similar results have also been obtained by Senoussi with different approximations and, therefore, different numerical factors.<sup>33</sup>

Just as for  $\chi_d(H_0^m)$ , our experimental values are roughly consistent with this result. The slight discrepancies between the data and the calculations are not surprising. First, the calculations are only approximate. Then, since our samples are not circular, the effects of the corners of the squares or rectangles might perturb the critical currents in the sample. It had been shown, indeed, by use of the Faraday technique, that flux penetration in a square sample is not as regular as in a circular one.<sup>34</sup>

One should point out that this analysis clearly establishes that the length scale of the critical currents in an epitaxial  $\text{YBa}_2\text{Cu}_3\text{O}_7$  film is of the order of the in-plane film size. This is, of course, not the case in granular films.

#### IV. HYSTERESIS LOOP AND REMANENT MAGNETIZATION STUDIES

##### A. Results

Detailed studies of the hysteresis loops can be performed for different values of the maximum applied field  $H_0^m$  as shown in Fig. 5. This figure shows typical loops obtained at 10 K for  $B_0^m$  in the range 0–6 T. They were obtained with typical field sweeping rates  $\sim 5$  mT/s<sup>-1</sup>.

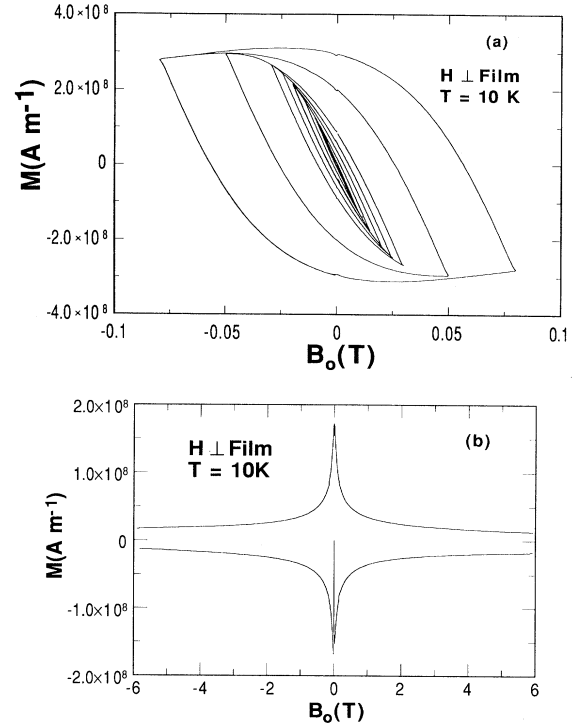


FIG. 5. Typical hysteresis loops for increasing applied fields,  $d = 150$  nm. (a) Small maximum applied fields. Note that  $\chi_d(H_0^m)$  is the same for all loops; (b) typical high-field hysteresis loop.

We have shown previously that the differential reverse susceptibility does not depend on  $H_0^m$ . This is not the case for the remanent magnetization  $M_r$  (or trapped flux), which increases with  $H_0^m$  as long as it has not reached a saturation value. Figure 6 shows a typical curve of  $M_r$  as a function of  $H_0^m$  either with semi-log or with log-log scales.

One can define from these curves a threshold field  $B_1$  for the onset of a measurable remanent magnetization  $M_r$ . The definition of this field depends primarily on the sensitivity of the experiment. In our case,  $B_1$  is defined by

$$\frac{M_r(B_1)}{M_r^{\text{sat}}} = 10^{-3}.$$

One can also define a saturation field  $B_2$  corresponding to the onset of the saturated value of the remanent magnetization  $M_r$ :  $B_0 = B_2$  for  $M_r = M_r^{\text{sat}}$ . In the case of the simple Bean model, with  $J_c$  independent of  $B$ ,  $B_2$  is expected to be twice the field  $B^*$  for full penetration of the vortices toward the center of the film (see, for example, Ref. 35). For  $B_1 < B_0^m < B_2$ , the semi-log plot shows that  $M_r$  is increasing with  $B_0^m$ , with a law involving  $(H_0^m)^2$ .

Figure 7(a) shows the curves of the normalized remanent magnetization  $M_r/M_r^{\text{sat}}$  for films of different thicknesses. The curves are displaced toward increasing field for increasing thickness. Figure 7(b) shows  $B_1$  as a

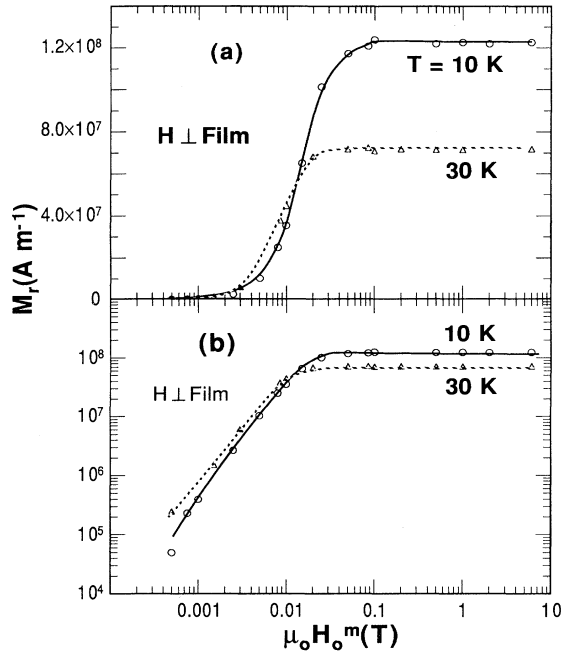


FIG. 6. Remnant magnetization  $M_r$  as a function of the maximum applied field  $\mu_0 H_0^m$ .  $H \perp$  film,  $d = 100$  nm. ( $\circ$ ):  $T = 10$  K, ( $\triangle$ ):  $T = 30$  K. (a) Semi-log plot; (b) log-log plot showing that, in low fields, laws approximately in  $(H_0^m)^2$  are followed.

function of thickness.  $B_1$  seems to increase approximately linearly with  $d$  for small thicknesses and to saturate for higher values of  $d$ . Figure 7(c) shows the field  $B_2$  as a function of  $d$ . The tendency for  $B_2$  is similar to that noted for  $B_1$ .

Figure 8 shows the saturated value of the remanent magnetization as a function of  $d$ . This curve shows a maximum for  $d$  100 nm and a decrease above.

### B. Discussion

Let us first discuss the general behavior of the curve  $M_r(H_0^m)$ . In the case of an infinite cylinder of radius  $R$  in a parallel applied field, the remanent magnetization is saturated only for a field  $2H^*$  ( $H^* = J_c R$ ). For  $H_0^m < H^*$ ,  $M_r$  can be worked out from the Bean article<sup>7</sup> and is found to be

$$M_r = \frac{(H_0^m)^2}{2H^*} - \frac{(H_0^m)^3}{4H^{*2}} \quad \text{for } H_0^m < H^* .$$

Our results, which show a  $(H_0^m)^2$  dependence in fields quite smaller than the full penetration field would agree roughly with the Bean model. However, the Bean model clearly should not apply in this case because of the large demagnetizing field effects. For the same reason, the Bean formula which predicts the saturated value of the remanent magnetization  $M_r = H^* / 3 = J_c R / 3$ , is dubious. Several authors have examined the problem of the critical state of a circular film or disk in a perpendicular applied field in order to clarify this point. The basic problem lies in the critical-state equation,

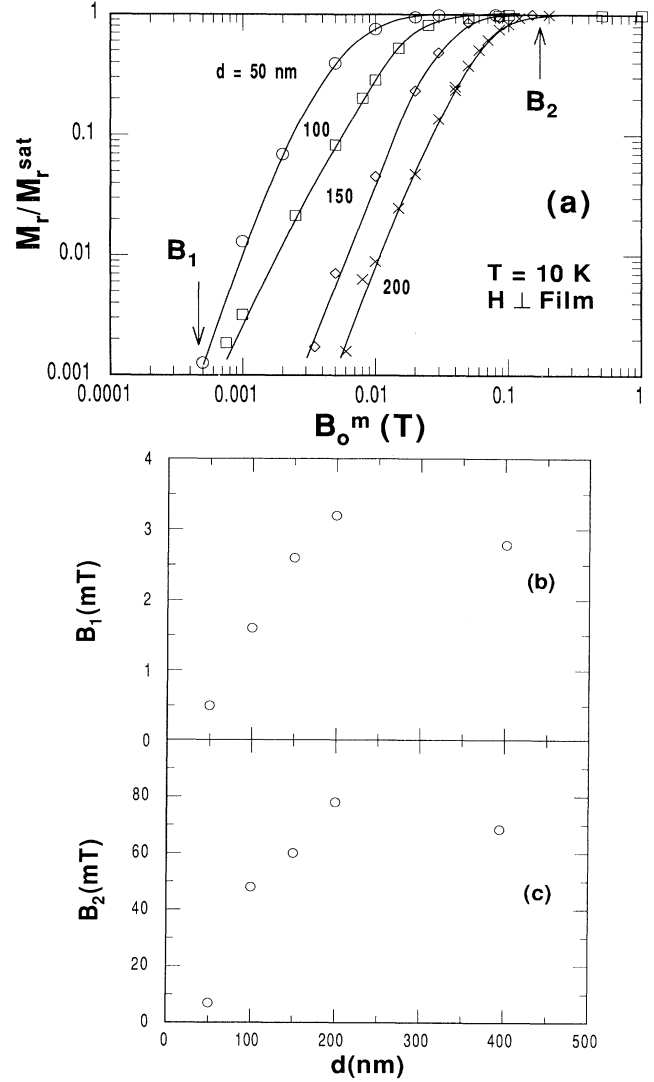


FIG. 7. Remanent-magnetization studies for different thicknesses  $d$ .  $T = 10$  K,  $H \perp$  film. (a)  $M_r / M_r^{\text{sat}}$  as a function of  $B_0^m$ .  $M_r^{\text{sat}}$  is the saturated remanent magnetization.  $d = 50$  nm ( $\circ$ ), 100 nm ( $\square$ ), 150 nm ( $\diamond$ ), 200 nm ( $\times$ ). (b) Field  $B_1$  for the onset of the remanent magnetization defined with the criterion  $M_r(B_1)M_r^{\text{sat}} = 10^{-3}$ . (c) Field  $B_2$  corresponding to the saturation  $M_r$  as a function of thickness.

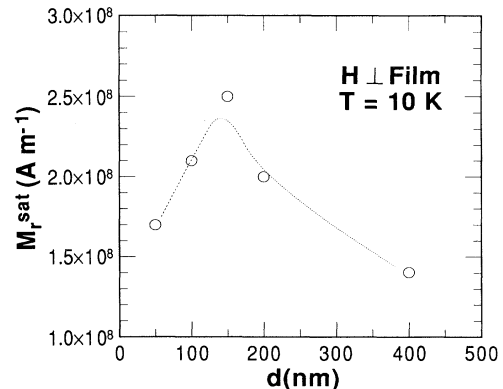


FIG. 8. Saturated remanent magnetization  $M_r^{\text{sat}}$  as a function of thickness.  $H \perp$  film,  $T = 10$  K.

$$\mu_0 \mathbf{J}_c = \nabla \times \mathbf{B}_0$$

which becomes in this geometry,

$$\mu_0 J_{c\phi}(r) = \frac{\partial B_r}{\partial z} - \frac{\partial B_z}{\partial r},$$

where  $J_{c\phi}$  is the critical current which flows in the circumferential direction,  $B_z$  is the longitudinal component of  $\mathbf{B}$ , parallel to the applied field  $\mathbf{H}_0$ , while  $B_r$  is a radial component which does not vanish. All models lead to numerical calculations for the evaluation of the magnetization. They are based on the decomposition of the critical current distribution in concentric current loops. More refined models take into account some field dependence of the critical current  $J_c$ . The first calculation by Frankel<sup>36</sup> predicted the field profile for a thick sample, with a thickness much larger than the London penetration depth. Further developments were performed by Däumling and Larbalestier<sup>37</sup> who obtained for the same case, field profiles for several values of the geometrical factor  $R/d$ . Conner and Malozemoff<sup>38</sup> have calculated the remanent magnetization, using the Kim<sup>39</sup> formula for the field dependence of  $J_c$  ( $J_c = \alpha/H_0 + C$ ). They show that the Bean formula  $M_r = J_c R/3$  is approximately followed for thin samples ( $d \leq C^2/\alpha$ ). Unfortunately, the calculations were not performed for thin films, but only for bulk samples ( $R/d \leq 15$ ). More recently, Theuss, Forkl, and Kronmüller<sup>40</sup> used the same model in the case of thin films in order to predict the flux-density profiles when increasing the field from a zero-field-cooled initial state. But they did not calculate the remanent magnetization. As far as we know, no calculation of the remanent magnetization in a thin film ( $R/d \sim 10^4$ ) is available at the moment. One should note that the simple Bean formula would be correct if the critical current density was constant throughout the disk. However, the available theories establish that the critical current  $J_c$  is related mainly to the spatial variation across the film thickness of the radial component  $B_r$  of the field. Therefore, they show that the curvature of the vortices is very likely non-negligible. But models adapted for a film with a thickness smaller than the London penetration depth should also take into account surface energies and local energies associated with vortex bending.

In the absence of numerical calculations, one has to use simple evaluations. For example, the applied field  $H_2$  which induces a saturation of the remanent magnetization can be estimated roughly on the basis of a model<sup>33</sup> similar to that of Angadi *et al.*<sup>32</sup> In this model, one calculates the field created at the center of the film by a distribution of annular critical currents. The full penetration field can then be evaluated by assuming that the critical currents circulate through the whole sample. One obtains  $H_2 = \gamma J_c d$ , where  $\gamma$  is a factor of the order of unity. This predicts in a first approximation, and below some characteristic thickness, approximately a linear variation of  $H_2$  with the thickness for constant critical currents. Our results do show a linear increase of  $H_2$  with thickness for thicknesses smaller than several hundreds of nm [Fig. 7(c)].

The increase of the threshold value  $B_1$  with  $d$  is related

to a decrease of the demagnetizing field effects for increasing thickness. It should be compared with the apparent lower critical field,

$$\mu_0 H_{c1}^{(a)} = \mu_0 \epsilon H_{c1} = \mu_0 \frac{\pi}{4} \frac{d}{R} H_{c1}.$$

One should note that  $B_1$  ( $\sim 10^{-3}$  T) is much larger than  $\mu_0 H_{c1}^{(a)}$  which is expected to be  $\sim 10^{-5}$  T at 10 K. We believe that this discrepancy might be due to the experimental inaccuracy. The experiment is probably not sensitive enough to detect the first trapped vortices. However, one cannot exclude other effects, such as barrier-type phenomena, preventing the penetration of vortices in low fields.

One can try to evaluate the critical current from the magnetic measurements and compare the values obtained from the saturated remanent magnetization through the conventional Bean formula ( $J_c^{(1)} = 3M_r/R$ ) and from the values of the full penetration field  $H_2$  dependent on the thickness ( $J_c^{(2)} \sim H_2/d$ ). Figure 9 shows the curves of  $J_c^{(1)}$  and  $J_c^{(2)}$  as a function of thickness. The agreement between both sets of data is satisfactory. One first notes that the order of magnitude of  $J_c^{(1)}$  and  $J_c^{(2)}$  is consistent with transport data. Further, these results seem to indicate that the critical current is decreasing with increasing thickness above roughly 100 nm. One should recall that the films studied here, with different thicknesses, have the same values of the room-temperature resistivity and neighboring critical temperatures above 100 nm. Therefore, the decrease of the critical current has to be associated with a decrease of the pinning force on the vortices not related to gross crystal quality difference between the samples. Such a mechanism could account only for the decrease of  $J_c$  below roughly 100 nm. Above 100 nm, the decrease of  $J_c$  could suggest that a surface pinning mechanism could be dominant. Such mechanisms related either to the film surface or to the film-substrate interface have been invoked previously.<sup>41</sup> However, they apply rather to the geometry of surfaces parallel to the vortices,<sup>5,6</sup> which is not the case here. On the other hand, recent results have established that  $\text{YBa}_2\text{Cu}_3\text{O}_7$  thin

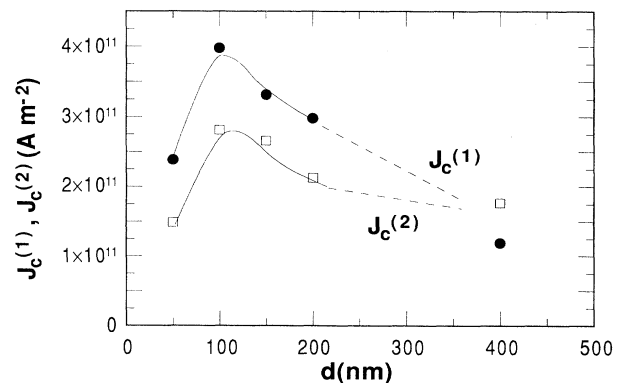


FIG. 9. Critical current as a function of thickness.  $J_c^{(1)}$  is evaluated from the Bean formula,  $J_c^{(1)} = 3M_r^{\text{sat}}/R$ ,  $J_c^{(2)}$  is calculated from the saturation field  $B_2 = \mu_0 H_2$ ;  $J_c^{(2)} \sim H_2/d$ .

films, elaborated by laser ablation or by sputtering, show a large concentration of screw dislocations.<sup>42–45</sup> Furthermore Mannhart *et al.* have shown that these dislocations act as pinning centers since the critical current  $J_c$  increases with their density.<sup>46</sup> It is not unlikely that this density depends on the thickness of the film. Results of Ref. 43 may indicate, indeed, a decrease of the screw dislocation density with increasing thickness. Further work should involve studies on the same films of structural and physical properties in order to corroborate this analysis.

## V. THICKNESS DEPENDENCE OF THE IRREVERSIBILITY LINE

### A. Results

The irreversibility line has been obtained from the hysteresis loops, as shown in Fig. 10. The field corresponding to the zero value of the irreversible magnetization at a given temperature  $T$  has been defined as  $B_{\text{irr}}(T)$ . This definition of  $B_{\text{irr}}$  depends on the choice of a magnetization criterion related to the experimental sensitivity. In our case, this criterion was  $100 \text{ emu/cm}^{-3}$  for all samples.

In order to get some insight into the mechanism governing the irreversibility line, we have also considered the field dependence of the pinning force,  $F_p = J_c B$ . For that, we have assumed that  $J_c$  is proportional to the measured irreversible magnetization  $M$ . The internal field  $B$  can be evaluated through

$$B = \mu_0(H_0 + H_d + M),$$

where  $H_0$  is the applied field and  $H_d$  the demagnetizing field. Since in the case of a thin film in perpendicular applied fields,  $H_d \simeq -M$ , one can assume

$$F_p = J_c B \sim MB_0 \quad (B_0 = \mu_0 H_0).$$

$F_p$  shows in all cases a maximum as a function of  $B$  at a value  $F_p^{\text{max}}$  and vanishes at  $B_0 = B_{\text{irr}}$ . Figure 11 shows the curve of the reduced value  $F_p/F_p^{\text{max}}$  as a function of the reduced field,  $b = B_0/B_{\text{irr}}$ , for temperatures between

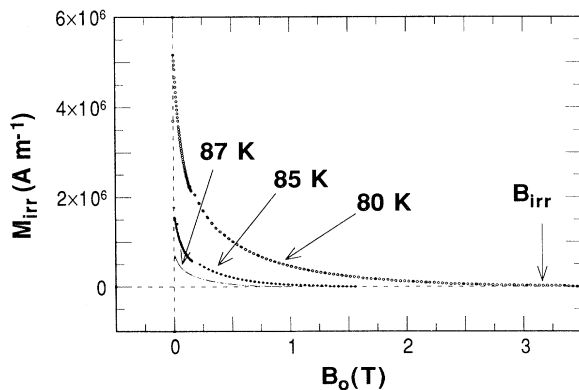


FIG. 10. Typical results for the reverse branch of the hysteresis loop at temperatures close to  $T_c$ .  $d = 400 \text{ nm}$ ,  $H \perp$  film.

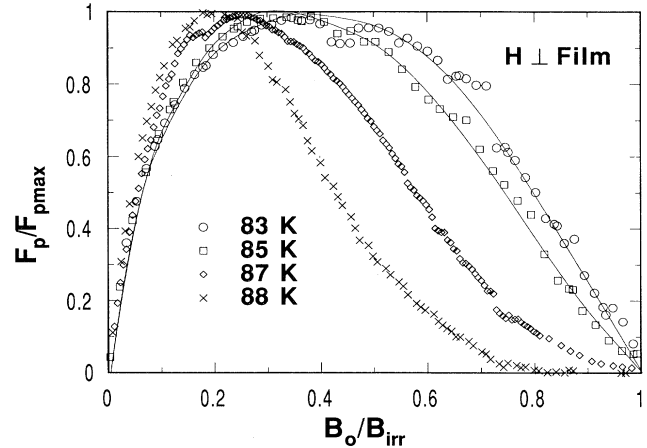


FIG. 11. Normalized pinning force ( $F_p/F_p^{\text{max}}$ ) as a function of the normalized field  $B_0/B_{\text{irr}}$ .  $F_p$  is evaluated from  $F_p \sim MB_0$ .  $F_p^{\text{max}}$  is the maximum value of the pinning force.  $H \perp$  film,  $d = 200 \text{ nm}$ .

83 K and  $T_c$ . These data show clearly that scaling laws, as first obtained by Kramer,<sup>47</sup> are not obeyed in the vicinity of  $T_c$ , since the curves are not superimposed. This means that if one fits  $F_p/F_p^{\text{max}}$  by

$$\frac{F_p}{F_p^{\text{max}}} = Kb^p(1-b)^q,$$

the exponents  $p$  and  $q$  are found to be temperature dependent, as shown in Fig. 12.

In conventional superconductors, temperature-independent values of  $\frac{1}{2}$  and 2 for  $p$  and  $q$ , respectively, were often found.<sup>47</sup> They were attributed to a pinning mechanism involving a shear of the vortex lattice around pinning centers. This model is similar to the collective pinning mechanism of Ref. 20. At temperatures below  $\sim 82 \text{ K}$ , our results are not inconsistent with such a model, within the experimental accuracy. At higher tempera-

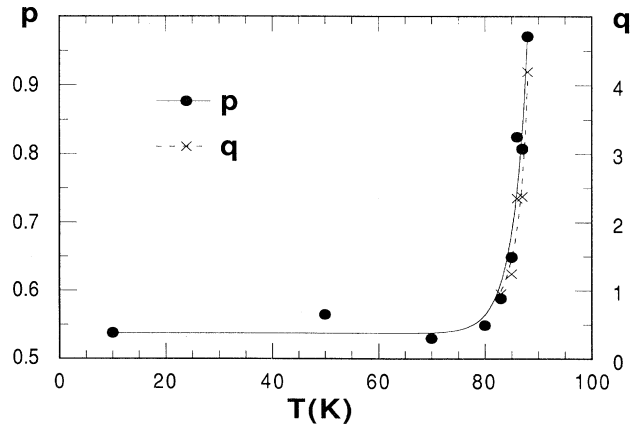


FIG. 12. Exponents  $p$  and  $q$  of the law  $F_p \sim (B_0/B_{\text{irr}})^p(1-B_0/B_{\text{irr}})^q$  as a function of temperature. Same sample as for Fig. 11.



tures, both  $p$  and  $q$  are increasing with  $T$ . Comparatively large values of these exponents have also been found in  $\text{YBa}_2\text{Cu}_3\text{O}_7$  single crystals.<sup>48</sup> One should note that the increase of  $p$  and  $q$  above  $\sim 80$  K may be due to large flux creep phenomena in the case of  $\text{YBa}_2\text{Cu}_3\text{O}_7$ .

Figure 13(a) shows the irreversibility line as obtained from the zero of the irreversible magnetization for different thicknesses. Independent of the thickness,  $B_{\text{irr}}$  follows a law of the type

$$B_{\text{irr}} \sim (1 - T/T_c)^n,$$

with an exponent  $n$  found to lie between 1.1 and 1.3. This exponent is clearly smaller than the value of 1.5 found in previous experiments.<sup>8,9,49</sup> It is also smaller than the values found recently on untwinned  $\text{YBa}_2\text{Cu}_3\text{O}_7$  single crystals, either by mechanical<sup>50</sup> or by electrical measurements.<sup>51</sup> This is not surprising since the films are very likely twinned. One should note that while our values of  $B_{\text{irr}}$  are similar to the values obtained by Koch *et al.* on epitaxial thin films,<sup>17</sup> they are systematically

smaller than values obtained on bulk single crystals.<sup>50,52,53</sup> This is corroboration that size effects may play a role on the value of  $B_{\text{irr}}$ . Similar results on the thickness dependence of the irreversibility line had been found by Civale, Worthington, and Gupta<sup>54</sup> by an ac-susceptibility technique, although our results seem to correspond to smaller values of  $B_{\text{irr}}$  for similar thicknesses.

Figure 13(b) shows that in our case,  $B_{\text{irr}}$  follows approximately a square-root law as a function of thickness:

$$B_{\text{irr}} \left( \frac{T}{T_c} \right) \sim d^{1/2}.$$

## B. Discussion

Although a large theoretical effort has been made on the mechanisms at the origin of the irreversibility line, little is known about size effects. One may first consider vortex-lattice melting theories, such as the model proposed by Nelson and Seung.<sup>11</sup> This model assumes that fluctuations in the vortex lattice are highly anisotropic and extend along the direction of the magnetic field. The longitudinal correlation length associated with these fluctuations  $\xi_{\parallel}$ , parallel to  $B$ , is then much larger than the transverse one,  $\xi_{\perp}$ . These correlation lengths are increasing with  $T$  and expected to diverge at a temperature corresponding to a three-dimensional melting transition. But, in finite samples, when  $\xi_{\parallel}$  becomes comparable to the sample size, a two-dimensional melting transition is expected to take place, therefore, at a temperature lower than the three-dimensional transition. Such a model should clearly predict a thickness dependence of the melting line for thin films in perpendicular fields. In fact, this has been worked out by Yeh.<sup>55</sup> The two-dimensional melting temperature was, indeed, found to increase with increasing thickness. Numerical values were obtained in the case of  $\text{YBa}_2\text{Cu}_3\text{O}_7$  for thicknesses of 200 and 2000 nm, respectively. A factor of roughly 2 was found at  $T/T_c \simeq 0.92$  for these two values. This is smaller, but comparable to our experimental results.

However, one may wonder if a model of vortex-lattice melting applies to the irreversibility line in thin films. The presence of a large density of pinning centers should be taken into account and models involving depinning processes should be examined. Let us consider the model proposed by Feigelman *et al.*<sup>21</sup> In this case, the destruction of the long-range order of the vortex lattice by pinning centers is associated with the correlation volume with a characteristic length  $L_c$  parallel to the magnetic field. If  $L_c$  becomes comparable or larger than the sample dimension along  $B$ , then the vortex-lattice disorder becomes two dimensional.<sup>56</sup>  $L_c$  was estimated in Ref. 57 by means of the collective pinning theory of Ref. 21. Previous estimations of  $L_c$  yielded a value of 7 nm for pinning by oxygen vacancies at low temperatures.<sup>58</sup> Other pinning mechanisms could also be responsible for much larger values of  $L_c$ . Our results may support orders of magnitude as large as 100 nm. But further theoretical development based on this type of model would be desirable.

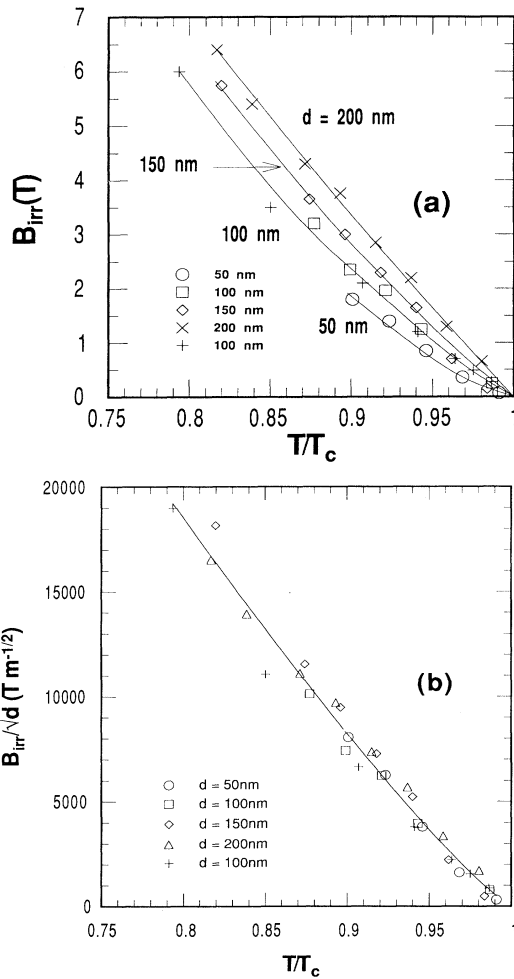


FIG. 13. (a) Irreversibility line obtained from the hysteresis loops for films of different thicknesses. (b)  $B_{\text{irr}}/\sqrt{d}$  as a function of normalized temperature  $T/T_c$ .

## VI. CONCLUSION

We have reported detailed studies of the magnetic properties of  $\text{YBa}_2\text{Cu}_3\text{O}_7$  epitaxial thin films in the superconducting state and have emphasized the dependence of these properties on the film thickness. We have shown that, in fields perpendicular to the films, the initial susceptibility is characteristic of a critical state for the outer part of the film. This initial susceptibility is always found equal to the differential susceptibility measured on the reverse branch of the hysteresis loop at the maximum applied field. Both quantities are decreasing with increasing thickness, as expected theoretically. The experimental values show that, in epitaxial films, the length scale of the critical current corresponds to the film size.

The remanent magnetizations studies establish that the characteristic fields  $B_1$  for the observable onset of the remanent magnetization (or trapped flux) and  $B_2$  for its saturation, increase with thickness approximately linearly for low thicknesses. This is expected for  $B_2$  on the basis of a simple electromagnetic estimation. We have also discussed the validity, in the perpendicular geometry, of the classical Bean formula for the calculation of the critical current. Our results indicate that in spite of the problems caused by the curvature of the vortices in this geometry, this formula might be approximately correct. It is now desirable that numerical calculations of the remanent magnetization with correct models should be performed. The evaluated critical current seems to decrease slightly with increasing thickness above roughly 100 nm. We have compared this result with the scanning tunneling microscopic studies which show clearly the presence of screw dislocations in  $\text{YBa}_2\text{Cu}_3\text{O}_7$  thin films and which indicate that these dislocations might be the dominant contribution to vortex pinning. Further work should involve studies of the critical current and of the screw dislocation density on the same samples, with various thicknesses.

We have found that the irreversible line is displaced toward higher fields with increasing thickness. Although this result is qualitatively expected, there is a lack of

theoretical calculations concerning thin films with a thickness comparable to the London penetration depth. We have, however, discussed these results in the framework of two models, the vortex-lattice melting and the collective pinning mechanism. In the first model, the vortex longitudinal correlation length associated with the elastic properties of the lattice has to be compared to the film thickness. In the second one, the characteristic length related to the pinning mechanism is the dominant physical parameter. Further studies are necessary to clarify this point.

We want to stress that our results corroborate the importance of shape demagnetizing field effects for the physical properties of superconducting thin films. Very low applied fields perpendicular to the samples may influence strongly these properties. One should especially be careful, in the course of studies in the presence of small oblique fields, that the perpendicular component only might control the vortex phenomenology and, therefore, many physical properties. Further work on the anisotropy of the magnetic properties establishing this point is presently in progress. On the other hand, in the high-field regime, demagnetizing field effects are expected to be negligible. Thickness effects have to be attributed to more intrinsic mechanisms. The angular dependence of the irreversibility line can then be studied by magnetization measurements and could be compared to other results.

## ACKNOWLEDGMENTS

The authors thank R. Buder for technical help for the vibrating-sample magnetometer and S. K. Agarwal for his participation with some measurements. We have benefited from some helpful discussions with I. A. Campbell, D. Caplin, J. Dumas, D. Feinberg, A. Malozemoff, S. Revenaz, S. Senoussi, and C. J. van der Beek. This work was partly supported by contracts from the Commission of the European Communities SCIENCE SC1-0038-CD and CI1-0340-F.

\*Present address: Institut für Physik, Universität Augsburg, Memminger Strasse 6, D 86135 Augsburg, Germany.

<sup>1</sup>J. G. Bednorz and K. A. Müller, *Z. Phys. B* **64**, 189 (1986).

<sup>2</sup>P. Chaudhari, R. H. Koch, R. B. Laibowitz, T. R. McGuire, and R. J. Gambino, *Phys. Rev. Lett.* **58**, 2684 (1987).

<sup>3</sup>M. Naito, R. H. Hammond, B. Oh, M. R. Hahn, J. W. P. Hsu, P. Rosenthal, A. F. Marshall, and M. R. Beasley, *J. Mater. Res.* **2**, 713 (1987).

<sup>4</sup>A. P. Malozemoff, in *Physical Properties of High Temperature Superconductors*, edited by D. M. Ginsberg (World Scientific, Singapore, 1989), p. 71.

<sup>5</sup>See, for example, H. Ullmaier, *Irreversible Properties of Type-II Superconductors*, (Springer, New York, 1975).

<sup>6</sup>See, for example, A. M. Campbell and J. E. Evetts, *Adv. Phys.* **21**, 199 (1972).

<sup>7</sup>C. P. Bean, *Phys. Rev. Lett.* **8**, 250 (1962); *Rev. Mod. Phys.* **36**, 31 (1964).

<sup>8</sup>K. A. Müller, M. Takashige, and J. G. Bednorz, *Phys. Rev. Lett.* **58**, 1143 (1987).

<sup>9</sup>Y. Yeshurun and A. P. Malozemoff, *Phys. Rev. Lett.* **60**, 2202 (1988); A. D. Malozemoff, T. K. Worthington, Y. Yeshurun, F. Holtzberg, and P. H. Kes, *Phys. Rev. B* **38**, 7203 (1988).

<sup>10</sup>M. P. A. Fisher, *Phys. Rev. Lett.* **62**, 1415 (1989).

<sup>11</sup>D. R. Nelson and H. S. Seung, *Phys. Rev. B* **39**, 9153 (1989).

<sup>12</sup>E. H. Brandt, *Phys. Rev. Lett.* **63**, 1106 (1989).

<sup>13</sup>D. S. Fisher, *Phys. Rev. B* **22**, 1190 (1980).

<sup>14</sup>J. M. Kosterlitz and D. J. Thouless, *J. Phys. C* **6**, 1181 (1973).

<sup>15</sup>E. H. Brandt, *Int. J. Mod. Phys. B* **5**, 751 (1991); *Physica C* **195**, 1 (1992).

<sup>16</sup>D. S. Fisher, M. P. A. Fisher, and D. A. Huse, *Phys. Rev. B* **43**, 130 (1991); R. E. Hetzel, A. Sudbø, and D. A. Huse, *Phys. Rev. Lett.* **69**, 518 (1992).

<sup>17</sup>R. H. Koch, V. Foglietti, W. J. Gallagher, G. Koren, A. Gupta, and M. P. A. Fisher, *Phys. Rev. Lett.* **63**, 1511 (1989).

<sup>18</sup>S. Gregory, C. T. Rogers, T. Venkatesan, X. D. Wu, A. Inam, and B. Dutta, *Phys. Rev. Lett.* **62**, 1548 (1989).

<sup>19</sup>P. W. Anderson and Y. B. Kim, *Rev. Mod. Phys.* **36**, 39 (1964).

- <sup>20</sup>A. I. Larkin and Yu N. Ovchinnikov, *J. Low Temp. Phys.* **34**, 409 (1979).
- <sup>21</sup>M. J. Feigelman, V. B. Geshkenbein, A. I. Larkin, and V. M. Vinokur, *Phys. Rev. Lett.* **63**, 2303 (1989); M. V. Feigelman and V. M. Vinokur, *Phys. Rev. B* **41**, 8986 (1990).
- <sup>22</sup>R. Buder, J. Dumas, C. Escribe-Filippini, H. Guyot, C. J. Liu, J. Marcus, S. Revenaz, and C. Schlenker, in *Studies of High Temperature Superconductors*, edited by A. V. Narlikar (Nova Science, New York, 1990), p. 223.
- <sup>23</sup>C. Schlenker, J. Dumas, C. J. Liu, and S. Revenaz, in *Chemistry of High Temperature Superconductors*, edited by C. N. R. Rao (World Scientific, Singapore, 1991), p. 484; C. Schlenker, C. J. Liu, R. Buder, J. Schubert, and B. Stritzker, *Physica C* **180**, 148 (1991).
- <sup>24</sup>C. J. Liu, S. K. Agarwal, R. Buder, J. Schubert, and C. Schlenker, in *High  $T_c$  Superconductors Thin Films*, edited by L. Corraera (Elsevier, New York, 1992), p. 177.
- <sup>25</sup>J. Frohlingsdorf, W. Zander, and B. Stritzker, *Solid State Commun.* **67**, 965 (1988).
- <sup>26</sup>B. Stritzker, J. Schubert, U. Poppe, W. Zander, U. Krüger, A. Lubig, and C. Buchal, *J. Less-Common Met.* **164-165**, 279 (1990).
- <sup>27</sup>C. J. Liu, R. Buder, C. Schlenker, J. Schubert, W. Zander, and B. Stritzker, *J. Less-Common Met.* **164-165**, 1285 (1990).
- <sup>28</sup>See, for example, L. D. Landau and E. M. Lifshitz, *Electrodynamics of Continuous Media* (Pergamon, New York, 1960).
- <sup>29</sup>L. Krusin-Elbaum, A. P. Malozemoff, Y. Yeshurun, D. C. Cronemeyer, and F. Holtzberg, *Phys. Rev. B* **39**, 2936 (1989).
- <sup>30</sup>A. L. Fetter and P. C. Hohenberg, *Phys. Rev.* **159**, 330 (1967).
- <sup>31</sup>T. Schuster, M. R. Koblischka, H. Kuhn, B. Ludescher, M. Leghissa, M. Lippert, and H. Kronmuller, *Physica C* **196**, 373 (1992), and references therein.
- <sup>32</sup>M. A. Angadi, A. D. Caplin, J. R. Laverty, and Z. X. Shen, *Physica C* **177**, 479 (1991).
- <sup>33</sup>S. Senoussi, *J. Phys. III (France)* **2**, 1041 (1992).
- <sup>34</sup>P. Brüll, D. Kirchgässner, and P. Leiderer, *Physica C* **182**, 339 (1991).
- <sup>35</sup>M. Xu, *Phys. Rev. B* **44**, 2713 (1991).
- <sup>36</sup>D. J. Franke, *J. Appl. Phys.* **50**, 5402 (1979).
- <sup>37</sup>M. Däumling and D. C. Larbalestier, *Phys. Rev. B* **40**, 9350 (1989).
- <sup>38</sup>L. W. Conner and A. P. Malozemoff, *Phys. Rev. B* **43**, 402 (1991).
- <sup>39</sup>Y. B. Kim, C. F. Hempstead, and A. R. Strand, *Rev. Mod. Phys.* **36**, 43 (1964).
- <sup>40</sup>H. Theuss, A. Forkl, and H. Kronmuller, *Physica C* **190**, 345 (1992).
- <sup>41</sup>B. Roas, L. Schultz, and G. Saemann-Ischenko, *Phys. Rev. Lett.* **64**, 479 (1990).
- <sup>42</sup>M. Hawley, I. D. Raistrick, J. G. Beery, and R. J. Houlton, *Science* **251**, 1587 (1991).
- <sup>43</sup>Ch. Gerber, D. Anselmetti, J. G. Bednorz, J. Mannhart, and D. G. Schlom, *Nature (London)* **350**, 279 (1991).
- <sup>44</sup>H. P. Lang, T. Frey, and H. J. Güntherodt, *Europhys. Lett.* **15**, 667 (1991).
- <sup>45</sup>D. G. Schlom, D. Anselmetti, J. G. Bednorz, R. F. Broom, A. Catana, T. Frey, Ch. Gerber, H. J. Güntherodt, H. P. Lang, and J. Mannhart, *Z. Phys. B* **86**, 163 (1992).
- <sup>46</sup>J. Mannhart, D. Anselmetti, J. G. Bednorz, A. Catana, Ch. Gerber, K. A. Müller, and D. G. Schlom, *Z. Phys. B* **86**, 177 (1992).
- <sup>47</sup>E. J. Kramer, *J. Appl. Phys.* **44**, 1360 (1973).
- <sup>48</sup>J. N. Li, F. R. de Boer, L. W. Roeland, M. J. V. Menken, K. Kadowaki, A. A. Menovsky, J. J. M. Franse, and P. H. Kes, *Physica C* **169**, 81 (1990).
- <sup>49</sup>C. C. Almasan, M. C. de Andrade, Y. Dalichaouch, J. J. Neumeier, C. L. Seaman, M. B. Maple, R. P. Guertin, M. V. Kuric, and J. C. Garland, *Phys. Rev. Lett.* **69**, 3812 (1992).
- <sup>50</sup>D. E. Farrell, J. P. Rice, and D. M. Ginsberg, *Phys. Rev. Lett.* **67**, 1165 (1991).
- <sup>51</sup>H. Safar, P. L. Gammel, D. A. Huse, D. J. Bishop, J. P. Rice, and D. M. Ginsberg, *Phys. Rev. Lett.* **69**, 824 (1992).
- <sup>52</sup>L. Krusin-Elbaum, L. Civale, F. Holtzberg, A. P. Malozemoff, and C. Feild, *Phys. Rev. Lett.* **67**, 3156 (1991).
- <sup>53</sup>L. Civale, A. D. Marwick, T. K. Worthington, M. A. Kirk, J. R. Thompson, L. Krusin-Elbaum, Y. Sun, J. R. Clem, and F. Holtzberg, *Phys. Rev. Lett.* **67**, 648 (1991).
- <sup>54</sup>L. Civale, T. K. Worthington, and A. Gupta, *Phys. Rev. B* **43**, 5425 (1991).
- <sup>55</sup>N. C. Yeh, *Phys. Rev. B* **42**, 4850 (1990).
- <sup>56</sup>P. H. Kes and J. van der Berg, in *Studies of High Temperature Superconductors*, edited by A. V. Narlikar (Nova Science, New York, 1990), Vol. 5, p. 83.
- <sup>57</sup>C. J. van der Beek, P. H. Kes, M. P. Maley, M. J. V. Menken, and A. A. Menovsky, *Physica C* **195**, 307 (1992).
- <sup>58</sup>P. H. Kes, *Physica C* **185-189**, 288 (1991).